



Available online at www.sciencedirect.com

ScienceDirect

Mathematics and Computers in Simulation 182 (2021) 871–887

MATHEMATICS
AND
COMPUTERS
IN SIMULATION


www.elsevier.com/locate/matcom

Original articles

Periodic solutions, chaos and bi-stability in the state-dependent delayed homogeneous Additive Increase and Multiplicative Decrease/Random Early Detection congestion control systems[☆]

Lijun Pei*, Fanxin Wu

School of Mathematics and Statistics, Zhengzhou University, 450001 Zhengzhou, Henan, China

Received 29 December 2019; received in revised form 21 April 2020; accepted 1 June 2020

Available online 4 June 2020

Abstract

The combination of Additive Increase and Multiplicative Decrease (AIMD) congestion control and Random Early Detection (RED) queue as a whole congestion control system plays a key role in the overwhelming success of the Internet. Thus it is important to investigate the periodic oscillations and complicated dynamics of the state-dependent delayed homogeneous Additive Increase and Multiplicative Decrease/Random Early Detection (AIMD/RED) congestion control system and its modified version fully in this paper. Firstly employing the semi-analytical method called as the harmonic balance method with alternating frequency/time (HB-AFT) domain technique, the approximate analytical expressions of periodic solutions of the generalized homogeneous-flow Additive Increase and Multiplicative Decrease/Random Early Detection (AIMD/RED) system with state-dependent round-trip delay are considered. We compare them with the results of numerical simulations by WinPP, they agree very well with each other. It demonstrates that the method employed here is versatile, valid, simple and effective. Then to the end of improving its modeling and performance, we modify the above model by taking an easy approximate dropping function. Furthermore, for the modified delayed homogeneous system, the approximate analytical expressions of periodic solutions are obtained accurately, and some complex dynamics are also presented. Four kinds of bi-stability, i.e., the coexistence of chaos and Period-3 solution, that of Period-1 and Period-2 solutions, that of Period-2 and Period-2 solutions, that of Period-4 and Period-2 solutions are disclosed. And a route to chaos, i.e., Period Doubling bifurcation to chaos, and the window of Period-3 to chaos are also discovered. The periodic oscillation can reduce the link utilization, induce the TCP stream synchronization services and further congestion. Chaotic oscillation may result in collapse. Therefore, all complex dynamical phenomena found in this paper are harmful and should be avoided. The obtained results can be very helpful for the researchers to have a better understanding of the mechanism of the network congestion control system, and they can select the parameters properly to improve the network stability and performance.

© 2020 International Association for Mathematics and Computers in Simulation (IMACS). Published by Elsevier B.V. All rights reserved.

Keywords: AIMD/RED congestion control system; HB-AFT; Periodic solutions; Bi-stability; Chaos

[☆] This work was supported by the NNSF of China under the Grant Nos. 11972327, 11372282 and 10702065.

* Corresponding author.

E-mail address: peilijun@zzu.edu.cn (L. Pei).

1. Introduction

With its rapid development, the Internet becomes a more heterogeneous and diverse nonlinear giant system. Applications and users are growing while the resources in the network are limited, and heterogeneous networks are converging. User's demand for the quality of network service is getting higher and higher, and the problem of network congestion is becoming more and more serious in practical applications. Internet congestion, is a kind of network state with continuous overload, appearing when the user's demand for network resources exceeds its inherent capacity. This phenomenon can lead to an increase of packet loss. It may also result in loss of information, the increasing delays and even make the system collapse.

In order to effectively avoid network congestion, the end-to-end flow control mechanism was proposed by Jacobson [1], i.e., transmission control protocol (TCP), which is based on a sliding window mechanism and uses an additive increase and multiplicative decrease (AIMD) algorithm. To be specific, when congestion does not occur, the sender additively increases the transmission rate to survey for the unused bandwidth, and decreases its transmission rate exponentially (multiplicatively), which is the response to network congestion, the additive increase rate of TCP is one packet per round-trip time (rtt) and the multiplicative decrease ratio of TCP is half. For the sake of obtaining better quality of service performance, some active queue management (AQM) algorithms are proposed. The purpose of these algorithms is to detect the possible congestion at the routers early, and to inform the senders to take measures by randomly discarding or marking packets, so as to effectively avoid network congestion. AQM offers some algorithms, e.g., random early detection (RED) [2], random early marking (REM) [3], Drop Tail. RED is a famous AQM algorithm. When the packet arrives at the queue, if the average queue length is less than the minimum threshold, the packet enters the queue. With the increase of queue length, as the average queue length is between the minimum and the maximum threshold, the probability of packet dropping increases. When the average queue length is greater than the maximum threshold, and the probability reaches 1, the incoming packet is discarded. The three stages of dropping function are called as normal, congestion avoidance and congestion control. So its mechanism is to detect the occurrence of congestion by detecting the average queue length at the routers to suppress the global synchronization at the sources. Therefore, AIMD and RED are among the core of those congestion control mechanisms. Thus to the end of enhancing network stability and improving system performance, in the present paper, it is significant to study the periodic oscillations and complicated dynamics of the state-dependent delayed homogeneous AIMD/RED congestion control system and its modified version fully, this is our motivation of this paper.

The mathematical models of these algorithms were established, the stability and dynamics of the Internet congestion control system with time delay were widely investigated. For researchers, the deep insight of complex dynamics of the Internet congestion control system is an indispensable element for a good understanding of the control algorithms, and it is also useful to find novel algorithms. So there are many works about the dynamics and stability of the Internet congestion control system for the recent years. For the exponential RED algorithm with communication delay, the stability and direction of bifurcating periodic solution were investigated [4]. The authors studied the problem of Hopf bifurcation control for the congestion control model in a wireless access network with time delay [5]. The combination of the fluid-flow model for TCP congestion avoidance and various AQM schemes was investigated, moreover, they discovered oscillations and bifurcations via numerical means [6]. In addition, in [7], the authors researched the Hopf bifurcation and chaos of a kind of RED-AQM congestion control model with time delay, and they displayed that there is a critical value of time delay for the stability of the system. In order to study oscillatory dynamics induced by the time delay employing the Hopf bifurcation, the authors considered an n-dimensional internet congestion control system with ring topology. They obtained the quantitative relationship between the delay and oscillation induced by it via the method of multiple scales [8].

Time delay is ubiquitous in nature and human society. It means that the current tendency of the state depends on both the current and past states [9]. For the time delayed system, the characteristic equation near the equilibrium changes from polynomial equation to transcendental one, and the number of its roots increases from finite to infinite. The existence of the time delay makes the system dynamics more complicated, such as bifurcation, chaos and so on will occur. The performance of the network congestion control system has close relationship to its dynamical behaviors. Periodic oscillation can reduce the link utilization, induce the TCP stream synchronization services and further congestion. Chaotic oscillation may result in collapse. So it is significant to obtain the expressions of the

periodic solutions of the AIMD/RED control system and study the complex dynamical problems, however, those approximate expressions of state-dependent delayed systems are difficult to obtain.

There are two kinds of methods used in common to research the periodic solutions. One kind are general analytical methods, e.g., the center manifold theorem [10], multi-scale method [11–13], the perturbation method [14], etc. And the other are the combination of numerical and analytical methods, such as the harmonic balance (HB) method [15–17], high dimensional harmonic balance method [18], incremental harmonic balance method [19–21], the generalized harmonic balance (GHB) method [22], harmonic balance method with alternating frequency/time (HB-AFT) domain technique [23–27] and so on. However, some of them have limitations. For example, when the perturbation method is used, because the nonlinear term is a complex expression, it must be expanded in Taylor series at zero point to produce a linear term, and then find the solution by local disturbance. This method is very tedious. Due to the sharply weaker smoothness of their righthand, the classical retarded functional differential equation (RFDE) theory for the constant delayed differential equations is not suitable for the state-dependent delayed differential equations any more. Compared with other methods, the HB-AFT method is very different. It belongs to the frequency domain method, requires fewer integration and series expansion. It can be combined with the Fourier transform method quickly, so that the calculation speed of higher harmonic solutions is greatly improved. With the help of computer, the numerical iterative solution can be solved, and the higher-order harmonic solution with arbitrary accuracy can be obtained in theory.

The method of HB-AFT was first proposed by Yamachi in 1983 [23]. Then it was developed as a complete solution strategy for the periodic solution of dynamic systems by Kim and Noah [24,25], and next it is widely used to solve the periodic response of complex nonlinear system. Zhang and Chen [26] analyzed a fractional exponential and non-smooth system, combining the HB-AFT with the Floquet theory for the first time. They put forward the advantages of this method, for example, it can keep away from the analytical processing procedure. The HB-AFT method establishes the relationships of harmonic coefficients directly from the discrete time frequency characteristics, and it requires very little integration work in the solving process. Besides, in [27], for the sake of dealing with the complicated non-polynomial forces of the nonlinear piezoelectric mechanical systems, via the alternating frequency/time (AFT) domain progress, a set of implicit algebraic equations of harmonic balance (HB) method were established. And although the system has complex nonlinearities, the proposed method is very precise for strongly nonlinear piezoelectric mechanical systems. In the present paper, we also present the advantages of the HB-AFT method, and the approximate analytical expressions of periodic solutions of the AIMD/RED system with state-dependent delay are achieved accurately by the HB-AFT method, which is one of the contributions in this paper. Because the approximate analytical expressions of periodic solutions imply the whole spectral information of periodic solutions, moreover, they can help researchers to understand and control the problem of network congestion. In order to make the original system more practical, we modify it. At the same time, we find the approximate analytical periodic solutions show excellent agreement with those of the numerical solutions, and complex dynamics of the modified model, for example, the four kinds of bi-stability, i.e., the coexistence of chaos and Period-3 solution, that of Period-1 and Period-2 solutions, that of Period-2 and Period-2 solutions, that of Period-4 and Period-2 solutions. And a route to chaos for delay in some interval, i.e., Period Doubling bifurcation to chaos, and the window of Period-3 to chaos are also discovered with the variation of parameter T_p . It reveals that the variation of parameter is crucial to the dynamical phenomenon. To the author's knowledge, the periodic oscillation can induce TCP stream synchronization services and further congestion, and chaotic oscillation can result in collapse. Therefore, all the rich dynamical phenomena discovered in the AIMD/RED model can be very beneficial for the researchers to enhance the network stability indispensable for the health of the internet, by choosing the parameters properly. Hence, they are also the contributions of this paper.

The organization of this paper is as follows. In Section 2, we first introduce the AIMD/RED model as a state-dependent delayed system, then the HB-AFT method is introduced, and employ the HB-AFT method, some approximate analytical expressions of periodic solutions of the state-dependent delayed homogeneous AIMD/RED system are obtained. We compare these approximate analytical periodic solutions with the numerical simulations results by WinPP, they agree very well. It implies the validity, effectiveness, simplicity and accuracy of the method in this paper. In Section 3, we investigate the approximate analytical expressions of periodic solutions and the complex dynamics of its modified version in detail. Bi-stability and chaos are discovered. Finally, in Section 4, some conclusions are drawn from the investigation.

2. The congestion control system with state-dependent delay

2.1. A fluid-flow model of generalized homogeneous AIMD/RED system

Employing fluid-flow and stochastic differential equation analysis, a dynamic model of TCP behavior was presented firstly [28]. The authors extended the fluid-flow model for general AIMD (α, β) congestion control [29], and it is described by the following nonlinear differential equations,

$$\begin{cases} \frac{dW(t)}{dt} = \frac{\alpha}{R(t)} - \frac{2(1-\beta)}{1+\beta} W(t) \frac{W(t-R(t))}{R(t-R(t))} p(t-R(t)), \\ \frac{dq(t)}{dt} = \frac{N(t)W(t)}{R(t)} - C, \end{cases} \quad (1)$$

where $\alpha > 0$, $0 \leq \beta \leq 1$. In order to support heterogeneous traffic, the general AIMD congestion control system set the increase rate and decrease ratio employing a pair of parameters (α, β) . $W(t)$ represents the ensemble average of AIMD window size (packets) and $q(t)$ denotes the ensemble average of queue length (packets), they are positive and bounded variables. The round-trip time $R(t) = \frac{q(t)}{C} + T_p$, is the time needed for a packet to transmit from a certain source to a specific destination and return. C is the queue capacity (packets/s), T_p is the deterministic delay, which consists of the processing, propagation and the transmission delay. $N(t)$ represents the number of AIMD flows, $p(t)$ denotes the probability of a packet being marked or dropped and its value is in $[0, 1]$. When the capacity C is large, $N(t)$ can be assumed constant. With RED, the packet marking probability is made roughly proportional to average queue length, i.e., $p(t) = k_1 q(t)$ with $k_1 > 0$ [30]. Then Eq. (1) can be rewritten as

$$\begin{cases} \frac{dW(t)}{dt} = \frac{\alpha}{R(t)} - \frac{2(1-\beta)}{1+\beta} W(t) \frac{W(t-R(t))}{R(t-R(t))} k_1 q(t-R(t)), \\ \frac{dq(t)}{dt} = \frac{N(t)W(t)}{R(t)} - C. \end{cases} \quad (2)$$

For the convenience of calculation, we define $\tilde{t} = \omega t$. We still use the symbol t expresses the symbol \tilde{t} without confusion. Thus the equation becomes the following,

$$\begin{cases} \omega \dot{W}(t) = \frac{\alpha}{R(t)} - \frac{2(1-\beta)}{1+\beta} W(t) \frac{W(t-\omega R(t))}{R(t-\omega R(t))} k_1 q(t-\omega R(t)), \\ \omega \dot{q}(t) = \frac{N(t)W(t)}{R(t)} - C, \end{cases} \quad (3)$$

where dot denotes differentiation with respect to \tilde{t} , ω is the frequency of the periodic solution. The nonlinear terms of this system are

$$\begin{bmatrix} f_x \\ f_y \end{bmatrix} = \begin{bmatrix} \frac{\alpha}{R(t)} - \frac{2(1-\beta)}{1+\beta} W(t) \frac{W(t-\omega R(t))}{R(t-\omega R(t))} k_1 q(t-\omega R(t)) \\ -C + \frac{N(t)W(t)}{R(t)} \end{bmatrix}. \quad (4)$$

2.2. HB-AFT scheme

Firstly, based on the idea of harmonic balanced method, the periodic solutions and nonlinear terms of this system can be represented as the Fourier series expansions with the same orthogonal basis,

$$\begin{bmatrix} W(t) \\ q(t) \end{bmatrix} = \begin{bmatrix} a_{x0} \\ a_{y0} \end{bmatrix} + \sum_{k=1}^K \left[\begin{bmatrix} a_{xk} \\ a_{yk} \end{bmatrix} \cos(kt) - \begin{bmatrix} b_{xk} \\ b_{yk} \end{bmatrix} \sin(kt) \right], \quad (5)$$

$$\begin{bmatrix} f_x \\ f_y \end{bmatrix} = \begin{bmatrix} c_{x0} \\ c_{y0} \end{bmatrix} + \sum_{k=1}^K \left[\begin{bmatrix} c_{xk} \\ c_{yk} \end{bmatrix} \cos(kt) - \begin{bmatrix} d_{xk} \\ d_{yk} \end{bmatrix} \sin(kt) \right], \quad (6)$$

where a_{x0} , a_{y0} , c_{x0} and c_{y0} are the constants, a_{xk} , a_{yk} , c_{xk} and c_{yk} are the coefficients of cosine terms, b_{xk} , b_{yk} , d_{xk} and d_{yk} are the coefficients of sine terms, K represents the maximum number of selected harmonics.

Then, substituting Eqs. (5) and (6) into (3) and balancing the coefficients of harmonic terms in each order, $4K+2$ expressions about the harmonic coefficients are obtained,

$$g(P, Q) = 0. \quad (7)$$

The detailed expressions of algebraic equations g are described as follows.

For the constant terms,

$$\begin{bmatrix} g(1) \\ g(2) \end{bmatrix} = \begin{bmatrix} c_{x0} \\ c_{y0} \end{bmatrix} = \begin{bmatrix} 0 \\ 0 \end{bmatrix}. \quad (8)$$

For the sine terms,

$$\begin{bmatrix} g(4k-1) \\ g(4k) \end{bmatrix} = \omega k \begin{bmatrix} a_{xk} \\ a_{yk} \end{bmatrix} - \begin{bmatrix} d_{xk} \\ d_{yk} \end{bmatrix} = 0. \quad (9)$$

For the cosine terms,

$$\begin{bmatrix} g(4k+1) \\ g(4k+2) \end{bmatrix} = -\omega k \begin{bmatrix} b_{xk} \\ b_{yk} \end{bmatrix} - \begin{bmatrix} c_{xk} \\ c_{yk} \end{bmatrix} = 0, \quad (10)$$

where $k = 1, 2, 3, \dots, K$.

The coefficients of harmonics of periodic solutions and nonlinear terms can be expressed in the following vector form,

$$\begin{bmatrix} P \\ Q \end{bmatrix}^T = \begin{bmatrix} a_{x0} & a_{y0} & a_{x1} & a_{y1} & b_{x1} & b_{y1} & \cdots & a_{xK} & a_{yK} & b_{xK} & b_{yK} \\ c_{x0} & c_{y0} & c_{x1} & c_{y1} & d_{x1} & d_{y1} & \cdots & c_{xK} & c_{yK} & d_{xK} & d_{yK} \end{bmatrix}^T. \quad (11)$$

Note that the frequency ω is unknown, as a result, only by adding another condition on the phase of the first harmonic of the periodic solutions based on the fixed-phase method [31], i.e., $a_{x1} = 0$ or $b_{x1} = 0$ or $a_{y1} = 0$ or $b_{y1} = 0$, can we solve this equation $g = 0$, and take it as the additional equation,

$$g(4K+3) = 0. \quad (12)$$

The periodic solutions can be obtained by solving Eqs. (8)–(10) and (12). However, those algebraic equations are difficult to solve directly, thus the Newton–Raphson method for the iteration is employed in this paper. Moreover, we add the variable $P(4k+3) = \omega$. In order to solve the harmonic coefficients of $W(t)$, $q(t)$ by iteration, treat P as unknown variables, and consider Q as known variables. According to Eqs. (5), (6), (8)–(10) and (12), we can obtain the fixed point P^* of g by the Newton–Raphson iteration method, which can be performed as follows,

$$J^i(P^{i+1} - P^i) + g^i = 0, \quad (13)$$

$$\text{where } J = \frac{\partial g(P, Q)}{\partial P} + \frac{\partial g(P, Q)}{\partial Q} \frac{dQ}{dP}.$$

After the harmonic balance process, employing the alternating frequency/time (AFT) domain technique to get the values of Q and J in each step of iterations, is described in the following. Based on a supposed P , the discrete values of $W(t)$, $q(t)$ in the time domain are obtained by the Inverse Discrete Fourier Transform (IDFT), which can be expressed as the following,

$$\begin{bmatrix} W(n) \\ q(n) \end{bmatrix} = \begin{bmatrix} a_{x0} \\ a_{y0} \end{bmatrix} + \sum_{k=1}^K [\begin{bmatrix} a_{xk} \\ a_{yk} \end{bmatrix} \cos(\frac{2\pi kn}{N}) - \begin{bmatrix} b_{xk} \\ b_{yk} \end{bmatrix} \sin(\frac{2\pi kn}{N})], \quad (14)$$

where $n = 0, 1, 2, \dots, N$. $W(n)$, $q(n)$ represent the values of $W(t)$, $q(t)$ at the n th discrete time, respectively, i.e., the value at $n\frac{\tilde{T}}{N}$, where $\tilde{T} = 2\pi$, N is the number of discrete samples in the time domain.

Due to $W(n - \omega R(n)) = W_R(n)$, $q(n - \omega R(n)) = q_R(n)$, therefore,

$$\begin{aligned} W_R(n) &= a_{x0} + \sum_{k=1}^K [a_{xk} \cos(\frac{2\pi kn}{N} - k\omega R(n)) - b_{xk} \sin(\frac{2\pi kn}{N} - k\omega R(n))], \\ q_R(n) &= a_{y0} + \sum_{k=1}^K [a_{yk} \cos(\frac{2\pi kn}{N} - k\omega R(n)) - b_{yk} \sin(\frac{2\pi kn}{N} - k\omega R(n))], \end{aligned} \quad (15)$$

where $R(n) = T_p + \frac{q(n)}{C}$.

On the basis of Eqs. (14) and (15), we can get the discrete values of the nonlinear terms f_x and f_y , i.e.,

$$\begin{bmatrix} f_x(n) \\ f_y(n) \end{bmatrix} = \begin{bmatrix} f_x(W(n), q(n), W_R(n), q_R(n)) \\ f_y(W(n), q(n), W_R(n), q_R(n)) \end{bmatrix}. \quad (16)$$

The discrete values of f_x and f_y in the frequency domain are evaluated as Q employing the Discrete Fourier Transform (DFT), i.e.,

$$\begin{bmatrix} c_{x_0} \\ c_{y_0} \end{bmatrix} = \frac{1}{N} \sum_{n=0}^{N-1} \begin{bmatrix} f_x(n) \\ f_y(n) \end{bmatrix}, \quad (17)$$

$$\begin{bmatrix} c_{x_k} \\ c_{y_k} \end{bmatrix} = \frac{2}{N} \sum_{n=0}^{N-1} \begin{bmatrix} f_x(n) \\ f_y(n) \end{bmatrix} \cos\left(\frac{2\pi kn}{N}\right), \quad (18)$$

$$\begin{bmatrix} d_{x_k} \\ d_{y_k} \end{bmatrix} = -\frac{2}{N} \sum_{n=0}^{N-1} \begin{bmatrix} f_x(n) \\ f_y(n) \end{bmatrix} \sin\left(\frac{2\pi kn}{N}\right), \quad (19)$$

where $k = 0, 1, 2, \dots, K$.

In light of Eqs. (11), (13)–(19), the algebraic relationship between Q and P is established, which is obtained from the information transformation of time and frequency domains, and then by the iterations of Eq. (13), we can solve the fixed point P^* . The Jacobian matrix J can be calculated as

$$\left\{ \begin{array}{l} \frac{\partial g(1)}{\partial P(1)} = \frac{1}{N} \sum_{n=0}^{N-1} \frac{\partial f_1(n)}{\partial P}, \\ \frac{\partial g(2)}{\partial P(1)} = \frac{1}{N} \sum_{n=0}^{N-1} \frac{\partial f_2(n)}{\partial P}, \\ \dots \\ \frac{\partial g(4k-1)}{\partial P(4k-1)} = \omega k + \frac{2}{N} \sum_{n=0}^{N-1} \frac{\partial f_1(n)}{\partial P(4k-1)} \sin\left(\frac{2\pi kn}{N}\right), \\ \dots \\ \frac{\partial g(4k+2)}{\partial P(4k+2)} = -\omega k - \frac{2}{N} \sum_{n=0}^{N-1} \frac{\partial f_2(n)}{\partial P(4k+2)} \cos\left(\frac{2\pi kn}{N}\right), \\ \dots \\ \frac{\partial g(4K+2)}{\partial P(4K+3)} = -kb_{y_k} - \frac{2}{N} \sum_{n=0}^{N-1} \frac{\partial f_2(n)}{\partial P(4K+3)} \cos\left(\frac{2\pi kn}{N}\right), \end{array} \right. \quad (20)$$

where $k = 1, 2, \dots, K$.

The well combination of harmonic balance process and AFT process, and no approximation is introduced into the iterative process, so the iterations of Eq. (13) can generate more accurate fixed point P^* . The detailed iterative process of solving fixed point is as follows,

- (1) For a supposed initial value $P^{(0)}$, by employing Eqs. (8)–(10), (12) and (14)–(19), we can obtain the values of $g^{(0)}$ and $J^{(0)}$, respectively;
- (2) Iterate equation (13) once, the value of $P^{(1)}$ can be obtained;
- (3) Continue the above two steps, until the value of $\|P^{(i)} - P^{(i-1)}\|$ is less than a allowed error tolerance;
- (4) Return the value $P^{(i)}$ satisfying (3).

2.3. Numerical simulations

In this subsection, some examples are tested to verify the correctness and validity of the HB-AFT method employing the numerical simulations. The numerical simulations are obtained by the numerical simulation software of the nonlinear dynamics, WinPP. It integrates directly the governing equations by Runge–Kutta 4 method by WinPP. The numerical simulations have no relation to HB-AFT and verify its correctness and validity. The basic idea is to take the results obtained by WinPP as numerical solutions, compare the phase diagrams of numerical solutions with those of approximate analytical periodic solutions obtained by HB-AFT method, observe whether the diagrams are consistent or not.

Although the programming language of WinPP is simple, WinPP is powerful. The software is easy to operate and it is very suitable for numerical simulations of differential equations. By creating a program file with an ‘ode’ extension, the program file of this software mainly consists of two parts, the first part is the programming language of parameter evaluation marked by p , the second part is the writing program of system equations for numerical simulations. Take the first set of parameters as an example, the detailed program is presented in Appendix A.1. All

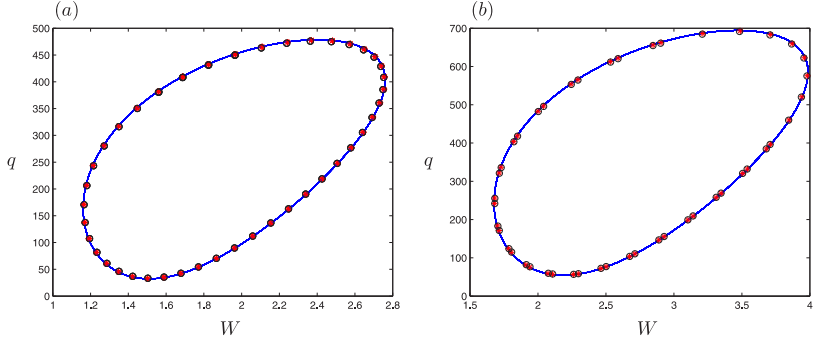


Fig. 1. The comparisons between the phase diagrams of lower order (blue \circ) and higher order HB-AFT method (red $*$) and those of numerical simulations (blue solid line) by WinPP. (a) under the set of parameters $T_p = 0.7225$, $C = 1000$, $N = 500$, $\alpha = 1$, $\beta = 0.5$, $k_1 = 0.002$, (b) under the set of parameters $T_p = 0.4703$, $C = 2210$, $N = 500$, $\alpha = 1.5$, $\beta = 0.6$, $k_1 = 0.0013$.

aspects of numerical simulations can be changed, except for the dimension and name of variables. It should also be noted that new files cannot be used without exiting. WinPP can find the equilibrium and draw the phase diagram (e.g. Fig. 5(a)), time histories (e.g. Fig. 5(b), (c)), Poincaré section (e.g. Fig. 9) and so on of the dynamical system, to analyze and verify various dynamical phenomena. Besides, if not mentioned, we will set the step size of WinPP $\Delta t = 0.0001$, the initial functions of WinPP are taken as $(W(s), q(s)) = (6, 600)$, $s \in [-R_{max}, 0]$. For the DDEs, we must set Max delay positive. When HB-AFT method is adopted, take harmonic number $K = 6$, the number of discrete samples in the time domain $N = 144$, iteration precision $\varepsilon = 10^{-16}$.

On the basis of the analysis in Section 2.2, we can obtain the Fourier coefficients and response frequency. Hence, for $T_p = 0.7225$, $C = 1000$, $N = 500$, $\alpha = 1$, $\beta = 0.5$, $k_1 = 0.002$, the analytical approximation of the Period-1 solution obtained by the HB-AFT method is the following,

$$\begin{aligned} W(t) &\approx 1.9630 - 0.7876 \sin(\omega t) + 0.0018 \cos(2\omega t) - 0.0756 \sin(2\omega t) \\ &\quad + 0.0023 \cos(3\omega t) - 0.0036 \sin(3\omega t) - 0.0001 \cos(4\omega t) \\ &\quad - 0.0006 \sin(4\omega t) + 0.0001 \cos(5\omega t) - 0.0001 \sin(5\omega t), \\ q(t) &\approx 259.0101 + 182.1625 \cos(\omega t) - 125.5455 \sin(\omega t) + 11.3294 \cos(2\omega t) \\ &\quad + 8.1175 \sin(2\omega t) - 1.0641 \cos(3\omega t) + 0.4887 \sin(3\omega t) \\ &\quad + 0.0677 \cos(4\omega t) - 0.1846 \sin(4\omega t) + 0.0258 \cos(5\omega t) \\ &\quad + 0.0244 \sin(5\omega t) - 0.0050 \cos(6\omega t) + 0.0023 \sin(6\omega t), \end{aligned}$$

where the response frequency is $\omega = 1.4960$ (see Fig. 1(a)).

According to the analysis in Section 2.2, the Fourier coefficients and response frequency are obtained. Consequently, for $T_p = 0.4703$, $C = 2210$, $N = 500$, $\alpha = 1.5$, $\beta = 0.6$, $k_1 = 0.0013$, the initial functions are taken as $(W(s), q(s)) = (4, 600)$, $s \in [-R_{max}, 0]$, the analytical approximation of the Period-1 solution obtained by the HB-AFT method reads

$$\begin{aligned} W(t) &\approx 2.8384 - 1.1365 \sin(\omega t) + 0.0054 \cos(2\omega t) - 0.1085 \sin(2\omega t) \\ &\quad + 0.0033 \cos(3\omega t) - 0.0048 \sin(3\omega t) - 0.0001 \cos(4\omega t) \\ &\quad - 0.0008 \sin(4\omega t) + 0.0001 \cos(5\omega t) - 0.0002 \sin(5\omega t), \\ q(t) &\approx 379.8152 + 261.8503 \cos(\omega t) - 178.5527 \sin(\omega t) + 16.0506 \cos(2\omega t) \\ &\quad + 12.0213 \sin(2\omega t) - 1.5766 \cos(3\omega t) + 0.6415 \sin(3\omega t) \\ &\quad + 0.1116 \cos(4\omega t) - 0.2627 \sin(4\omega t) + 0.0352 \cos(5\omega t) \\ &\quad + 0.0375 \sin(5\omega t) - 0.0075 \cos(6\omega t) + 0.0029 \sin(6\omega t), \end{aligned}$$

where the response frequency is $\omega = 2.3113$ (see Fig. 1(b)).

In Fig. 1, we take six and three order HB-AFT results (red $*$ and blue \circ). At the same time, the phase diagrams of numerical simulations (blue solid line) by WinPP are shown. It displays that the sixth-order HB-AFT results are in

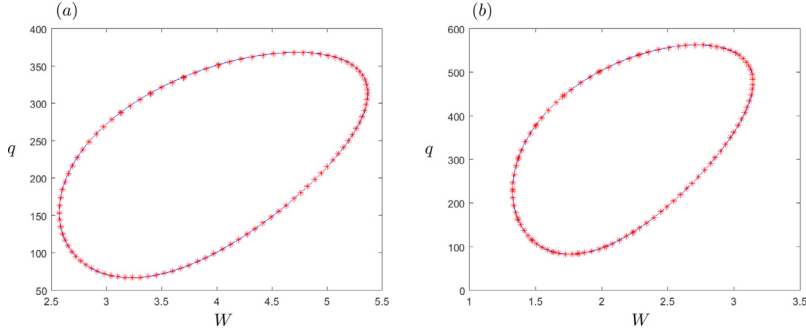


Fig. 2. Comparisons between the phase diagrams of the HB-AFT method and those of numerical simulations by WinPP, blue solid line: numerical simulations results; red *: the results of HB-AFT method. (a) for the parameters $T_p = 0.578$, $C = 1000$, $N = 200$, $\alpha = 2.5$, $\beta = 0.55$, $k_1 = 0.0015$, (b) for the parameters $T_p = 0.39926$, $C = 2000$, $N = 500$, $\alpha = 1.5$, $\beta = 0.465$, $k_1 = 0.0016$.

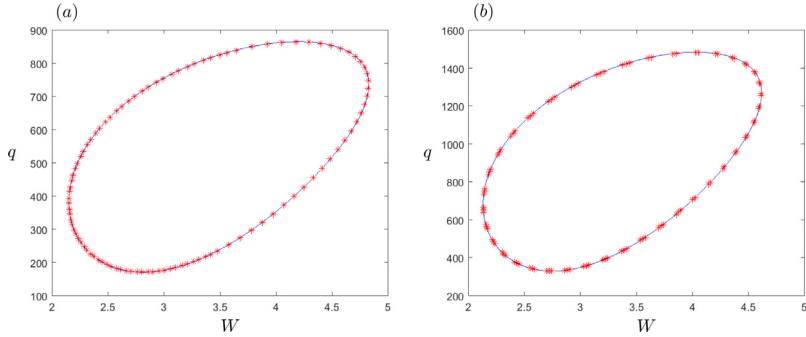


Fig. 3. Comparisons between the phase diagrams of the HB-AFT method and those of numerical simulations by WinPP, blue solid line: numerical simulations results; red *: the results of HB-AFT method. (a) for the parameters $T_p = 1.235$, $C = 1000$, $N = 500$, $\alpha = 2.6$, $\beta = 0.6$, $k_1 = 0.001$, (b) for the parameters $T_p = 0.715$, $C = 3000$, $N = 900$, $\alpha = 2.6$, $\beta = 0.6$, $k_1 = 0.0006$.

good agreement with those of the numerical simulations by WinPP. And we should pay attention that the third-order harmonic periodic solution is not as accurate as the sixth-order harmonic periodic solution. Consequently, to obtain more exact approximate analytical periodic solutions, we should not ignore the higher frequency information.

After solving Eq. (12), we can get the Fourier coefficients and response frequency. Therefore, we can obtain the following analytical approximation of the Period-1 solution by the HB-AFT method for $T_p = 0.578$, $C = 1000$, $N = 200$, $\alpha = 2.5$, $\beta = 0.55$, $k_1 = 0.0015$,

$$\begin{aligned} W(t) \approx & 3.9933 - 1.3849 \sin(\omega t) + 0.0210 \cos(2\omega t) - 0.1111 \sin(2\omega t) \\ & + 0.0026 \cos(3\omega t) - 0.0027 \sin(3\omega t) - 0.0007 \sin(4\omega t) \\ & + 0.0001 \cos(5\omega t) - 0.0001 \sin(5\omega t), \end{aligned}$$

$$\begin{aligned} q(t) \approx & 220.6693 + 125.6067 \cos(\omega t) - 81.6932 \sin(\omega t) + 6.2291 \cos(2\omega t) \\ & + 5.7964 \sin(2\omega t) - 0.6550 \cos(3\omega t) + 0.1175 \sin(3\omega t) \\ & + 0.0557 \cos(4\omega t) - 0.0770 \sin(4\omega t) + 0.0068 \cos(5\omega t) \\ & + 0.0132 \sin(5\omega t) - 0.0021 \cos(6\omega t) + 0.0001 \sin(6\omega t), \end{aligned}$$

where the response frequency is $\omega = 1.9436$ (see Fig. 2(a)).

According to the analysis of Section 2.2, we can obtain the Fourier coefficients and response frequency. Hence, when the initial functions are taken as $(W(s), q(s)) = (1, 600)$, $s \in [-R_{max}, 0]$, the following analytical approximation of the Period-1 solution is achieved by the HB-AFT method for $T_p = 0.39926$, $C = 2000$, $N = 500$,

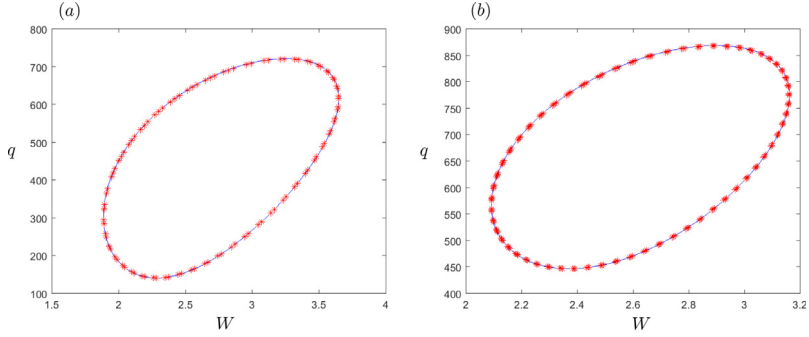


Fig. 4. Comparisons between the phase diagrams of the HB-AFT method and those of numerical simulations by WinPP, blue solid line: numerical simulations results; red *: the results of HB-AFT method. (a) for the parameters $T_p = 0.82$, $C = 1500$, $N = 600$, $\alpha = 1.6$, $\beta = 0.56$, $k_1 = 0.001$, (b) for the parameters $T_p = 0.58$, $C = 2500$, $N = 800$, $\alpha = 2.6$, $\beta = 0.5$, $k_1 = 0.0009$.

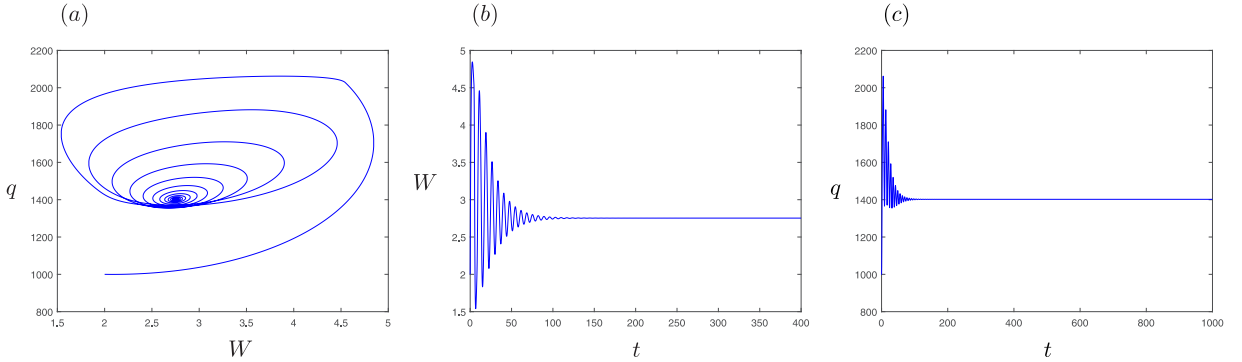


Fig. 5. (a) and (b), (c) correspond to the phase diagram and time histories of the system (21) for the parameter $T_p = 0.5$, respectively.

$$\alpha = 1.5, \beta = 0.465, k_1 = 0.0016,$$

$$W(t) \approx 2.2547 - 0.8967 \sin(\omega t) + 0.0184 \cos(2\omega t) - 0.0814 \sin(2\omega t)$$

$$+ 0.0017 \cos(3\omega t) - 0.0021 \sin(3\omega t) - 0.0008 \sin(4\omega t)$$

$$+ 0.0002 \cos(5\omega t) - 0.0001 \sin(5\omega t),$$

$$q(t) \approx 328.8090 + 201.0216 \cos(\omega t) - 127.9673 \sin(\omega t) + 11.0256 \cos(2\omega t)$$

$$+ 10.9094 \sin(2\omega t) - 1.3834 \cos(3\omega t) + 0.1292 \sin(3\omega t)$$

$$+ 0.1514 \cos(4\omega t) - 0.1708 \sin(4\omega t) + 0.0147 \cos(5\omega t)$$

$$+ 0.0383 \sin(5\omega t) - 0.0066 \cos(6\omega t) - 0.0004 \sin(6\omega t),$$

where the response frequency is $\omega = 2.8223$ (see Fig. 2(b)).

On the basis of the analysis in Section 2.2, the Fourier coefficients and response frequency can be obtained. Consequently, for $T_p = 1.235$, $C = 1000$, $N = 500$, $\alpha = 2.6$, $\beta = 0.6$, $k_1 = 0.001$, the following analytical approximation of the Period-1 solution is obtained by the HB-AFT method,

$$W(t) \approx 3.5241 - 1.3235 \sin(\omega t) + 0.0348 \cos(2\omega t) - 0.1094 \sin(2\omega t)$$

$$+ 0.0014 \cos(3\omega t) - 0.0019 \sin(3\omega t) + 0.0001 \cos(4\omega t)$$

$$- 0.0010 \sin(4\omega t) + 0.0002 \cos(5\omega t) - 0.0001 \sin(5\omega t),$$

$$\begin{aligned} q(t) \approx & 527.0399 + 293.1022 \cos(\omega t) - 180.9863 \sin(\omega t) + 14.2298 \cos(2\omega t) \\ & + 16.1292 \sin(2\omega t) - 1.8617 \cos(3\omega t) - 0.0859 \sin(3\omega t) \\ & + 0.2164 \cos(4\omega t) - 0.1843 \sin(4\omega t) + 0.0088 \cos(5\omega t) \\ & + 0.0474 \sin(5\omega t) - 0.0073 \cos(6\omega t) - 0.0020 \sin(6\omega t), \end{aligned}$$

where the response frequency is $\omega = 0.9298$ (see Fig. 3(a)).

In light of the analysis in Section 2.2, we can get the Fourier coefficients and response frequency. As a result, for $T_p = 0.715$, $C = 3000$, $N = 900$, $\alpha = 2.6$, $\beta = 0.6$, $k_1 = 0.0006$, the analytical approximation expression of the Period-1 solution obtained by the HB-AFT method reads,

$$\begin{aligned} W(t) \approx & 3.4074 - 1.2298 \sin(\omega t) + 0.0338 \cos(2\omega t) - 0.0962 \sin(2\omega t) \\ & + 0.0009 \cos(3\omega t) - 0.0015 \sin(3\omega t) + 0.0001 \cos(4\omega t) \\ & - 0.0008 \sin(4\omega t) + 0.0002 \cos(5\omega t), \\ q(t) \approx & 921.6546 + 488.4529 \cos(\omega t) - 298.7259 \sin(\omega t) + 22.2320 \cos(2\omega t) \\ & + 26.4353 \sin(2\omega t) - 2.8875 \cos(3\omega t) - 0.2659 \sin(3\omega t) \\ & + 0.3330 \cos(4\omega t) - 0.2594 \sin(4\omega t) + 0.0084 \cos(5\omega t) \\ & + 0.0683 \sin(5\omega t) - 0.0099 \cos(6\omega t) - 0.0035 \sin(6\omega t), \end{aligned}$$

where the response frequency is $\omega = 1.6169$ (see Fig. 3(b)).

According to the analysis in Section 2.2, we can get the Fourier coefficients and response frequency. So the following expression is the analytical approximation of the Period-1 solution achieved by the HB-AFT method for $T_p = 0.82$, $C = 1500$, $N = 600$, $\alpha = 1.6$, $\beta = 0.56$, $k_1 = 0.001$,

$$\begin{aligned} W(t) \approx & 2.7771 - 0.8721 \sin(\omega t) + 0.0084 \cos(2\omega t) - 0.0645 \sin(2\omega t) \\ & + 0.0016 \cos(3\omega t) - 0.0017 \sin(3\omega t) - 0.0003 \sin(4\omega t), \\ q(t) \approx & 436.2814 + 240.1597 \cos(\omega t) - 160.4124 \sin(\omega t) + 11.2726 \cos(2\omega t) \\ & + 9.5215 \sin(2\omega t) - 0.9904 \cos(3\omega t) + 0.2930 \sin(3\omega t) \\ & + 0.0638 \cos(4\omega t) - 0.1174 \sin(4\omega t) + 0.0111 \cos(5\omega t) \\ & + 0.0153 \sin(5\omega t) - 0.0023 \cos(6\omega t) + 0.0005 \sin(6\omega t), \end{aligned}$$

where the response frequency is $\omega = 1.3582$ (see Fig. 4(a)).

After solving Eq. (12), the Fourier coefficients and response frequency are obtained. Therefore, for $T_p = 0.58$, $C = 2500$, $N = 800$, $\alpha = 2.6$, $\beta = 0.5$, $k_1 = 0.0009$, the analytical approximation of the Period-1 solution obtained by the HB-AFT method reads

$$\begin{aligned} W(t) \approx & 2.6396 - 0.5337 \sin(\omega t) + 0.0125 \cos(2\omega t) - 0.0197 \sin(2\omega t) \\ & - 0.0002 \cos(3\omega t) - 0.0001 \sin(3\omega t) - 0.0001 \sin(4\omega t), \\ q(t) \approx & 661.6459 + 182.9147 \cos(\omega t) - 103.9305 \sin(\omega t) + 3.5814 \cos(2\omega t) \\ & + 6.3429 \sin(2\omega t) - 0.3226 \cos(3\omega t) - 0.1522 \sin(3\omega t) \\ & + 0.0261 \cos(4\omega t) - 0.0095 \sin(4\omega t) - 0.0008 \cos(5\omega t) \\ & + 0.0023 \sin(5\omega t) - 0.0001 \cos(6\omega t) - 0.0002 \sin(6\omega t), \end{aligned}$$

where the response frequency is $\omega = 2.0910$ (see Fig. 4(b)).

It follows that in the above approximate expressions of periodic solutions, all the coefficients of $\cos(\omega t)$ of $W(t)$ are 0, which is consistent with the condition on the phase of the first harmonic of the periodic solutions based on the fixed-phase method. We can perceive from the comparisons in the figures, the approximate analytical periodic solutions coincide with the results of numerical simulations by WinPP. It implies that the HB-AFT method can provide the accurate analytical approximate expressions for the state-dependent delayed congestion control system.

3. Its modified version

In the original system (1), the probability p is a linear function, which increases as the variable q increases. However, the upper bound of p should be 1, so the constraint of q is high. Then, in this paper, the original system

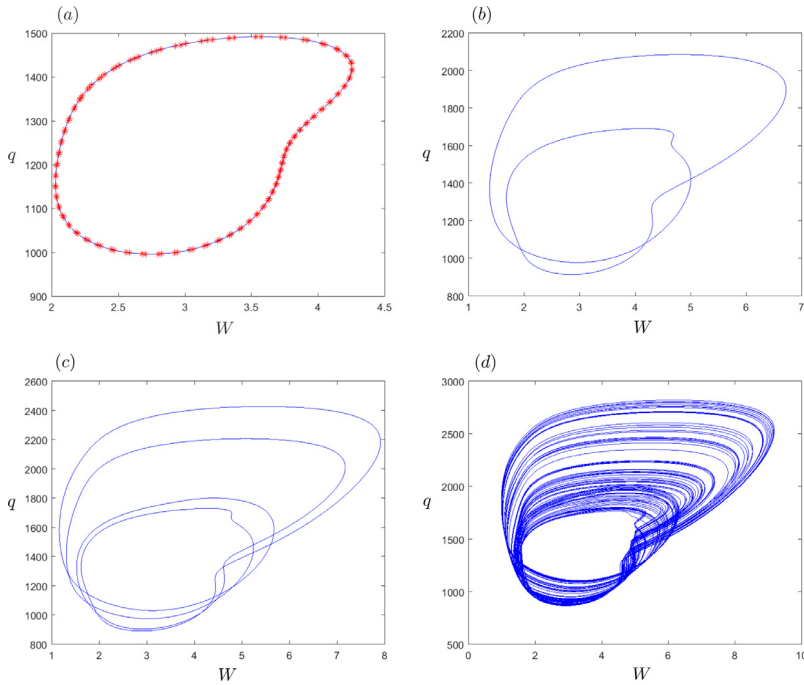


Fig. 6. Periodic and chaotic oscillations of the network congestion control system (21). (a) for $T_p = 1.3$, (b) for $T_p = 1.6$, (c) for $T_p = 1.69$, (d) for $T_p = 1.78$. And (a) is the comparison between the phase diagram of the HB-AFT method (red *) and that of numerical result (blue solid line) by WinPP.

(1) is improved by taking $p(t) = \frac{1}{2}(\tanh(k_1(q(t) - u)) + 1)$ [32]. The purpose is to make p have saturation effect and ensure that the system is more practical. Then Eq. (1) reads,

$$\begin{cases} \frac{dW(t)}{dt} = \frac{\alpha}{R(t)} - \frac{(1-\beta)}{1+\beta} W(t) \frac{W(t-R(t))}{R(t-R(t))} (\tanh(k_1(q(t-R(t)) - u)) + 1), \\ \frac{dq(t)}{dt} = \frac{N(t)W(t)}{R(t)} - C. \end{cases} \quad (21)$$

In this section, the complicated dynamical behaviors of the system (21) for feasible parameter regimes are further investigated through WinPP. Besides, if not mentioned, the step size of WinPP is taken as $\Delta t = 0.0001$. In order to explore the critical effect of parameter T_p on the dynamics of the model, the authors vary T_p , take it as bifurcation parameter, while holding the other parameters fixed as $C = 500$, $N = 600$, $\alpha = 10$, $\beta = 0.205$, $k_1 = 0.01$, $u = 1000$. When HB-AFT method is adopted, we take harmonic number $K = 6$, the number of discrete samples in the time domain $N = 144$, iteration precision $\varepsilon = 10^{-16}$.

Under the premise that the initial functions of WinPP are $(W(s), q(s)) = (2, 1000)$, $s \in [-R_{max}, 0]$, with the variation of parameter T_p , Hopf bifurcation accompanied by the occurrence of periodic oscillation emerges, and finally periodic solution will be transformed into chaos. For $0 < T_p < 1.133$, the system has an asymptotically stable equilibrium in Fig. 5. When $1.133 < T_p < 1.534$, the system exhibits a stable Period-1 response (blue solid line) in Fig. 6(a). Further, we can obtain the approximate analytical expression of the Period-1 solution for the parameter $T_p = 1.3$ through the HB-AFT method, the contents of which are presented in Appendix A.2. The comparison between the phase diagram of the HB-AFT method and that of numerical result is shown in Fig. 6(a), the red * represents the result of the HB-AFT method, the blue solid line represents the phase diagram obtained by WinPP. Obviously they show excellent agreement with each other.

As the parameter T_p increases slightly, for $1.534 < T_p < 1.6725$, a stable Period-2 solution occurs in Fig. 6(b). With the increase of parameter T_p , for $1.6725 < T_p < 1.7151$, a stable Period-4 solution takes place in Fig. 6(c), the Period Doubling sequence results in chaos ultimately for $1.726 < T_p < 1.859$ in Fig. 6(d). We have not yet obtained the approximate analytical expressions of the Period- m solution by the HB-AFT method, and we will continue to consider this work in the future.

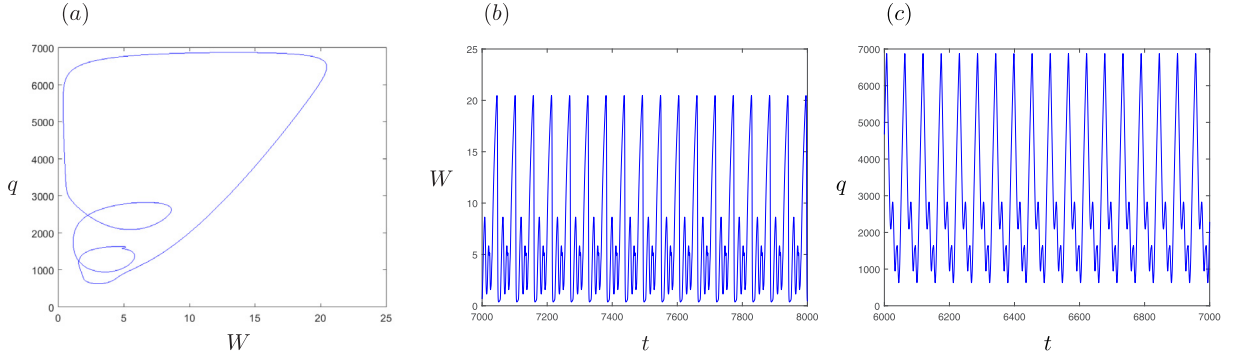


Fig. 7. (a) and (b), (c) correspond to the phase diagram and time histories of the system (21) for the parameter $T_p = 2.39$, respectively.

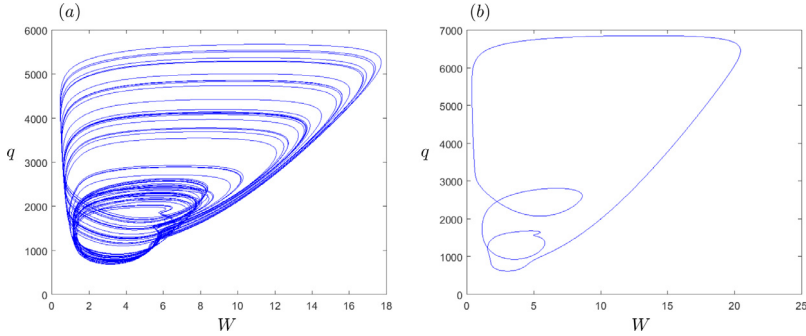


Fig. 8. The phenomenon of bi-stability of system (21) for the parameter $T_p = 2.415$. (a), (b) correspond to the initial functions $(W(s), q(s)) = (2, 1000)$ and $(W(s), q(s)) = (1, 700)$, $s \in [-R_{max}, 0]$, respectively.

When the parameter T_p continues to increase, for $1.859 < T_p < 2.41098$, a stable Period-3 solution appears in Fig. 7. As the parameter T_p increases further, for $2.41098 < T_p < 2.66$, the system exhibits chaos again in Fig. 8(a). Thus the window of Period-3 to chaos exists here [33]. Furthermore, when the initial functions and parameter are $(W(s), q(s)) = (1, 700)$, $s \in [-R_{max}, 0]$, and $T_p = 2.415$, obviously, there is a stable Period-3 solution in Fig. 8(b), i.e., the chaos coexists with the stable Period-3 solution. Fig. 9(a) is the bifurcation diagram generated by Poincaré section with respect to T_p of the route of Period Doubling bifurcation and the window of Period-3 to chaos corresponding to Fig. 6. All the discovered complex dynamical phenomena can be significant for researchers to control the parameters in a proper range to improve network performance.

We can also display another Period Doubling bifurcation to chaos and the phenomena of bi-stability, varying T_p , while fixing the other parameters as $C = 800$, $N = 2300$, $\alpha = 2.1$, $\beta = 0.29$, $k_1 = 0.05$, $u = 1000$. When HB-AFT method is adopted, we take harmonic number $K = 11$, the number of discrete samples in the time domain $N = 144$, iteration precision $\varepsilon = 10^{-16}$.

Under the premise that the initial functions of WinPP are $(W(s), q(s)) = (2, 1000)$, $s \in [-R_{max}, 0]$, for $0 < T_p < 2.67883$, the system has an asymptotically stable equilibrium, which is displayed in Fig. 10. For $2.67883 < T_p < 2.74201$, the system exhibits a stable Period-1 oscillation in Fig. 11(a). Besides, we obtain the approximate analytical expression of the Period-1 solution for the parameter $T_p = 2.71$ by the HB-AFT method, it is presented in Appendix A.2. At the same time, we compare the phase diagram of the HB-AFT method (red *) and that of numerical result (blue solid line) in Fig. 11(a). It follows that the result of HB-AFT method shows excellent agreement with that of numerical solution.

For $T_p \in (2.74201, 2.749)$, the stable Period-2 solutions occur in Fig. 11(b) and 12(a). While for $(W(s), q(s)) = (1, 700)$, $s \in [-R_{max}, 0]$, $T_p = 2.743$, a stable Period-1 solution also occurs in Fig. 12(b), i.e., the stable Period-2 solution coexists with the stable Period-1 solution. And Fig. 12(b) displays the comparison between the result of the HB-AFT method (red *) and numerical result (blue solid line). At the same time, we obtain the analytical

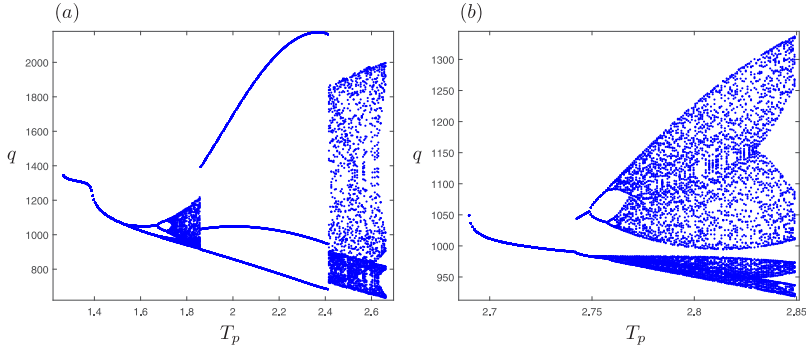


Fig. 9. The bifurcation diagrams generated by Poincaré section with respect to T_p of the route of Period Doubling bifurcation and the window of Period- 3 to chaos. (a), (b) correspond to Figs. 6, 7, 8(a) and 11, respectively.

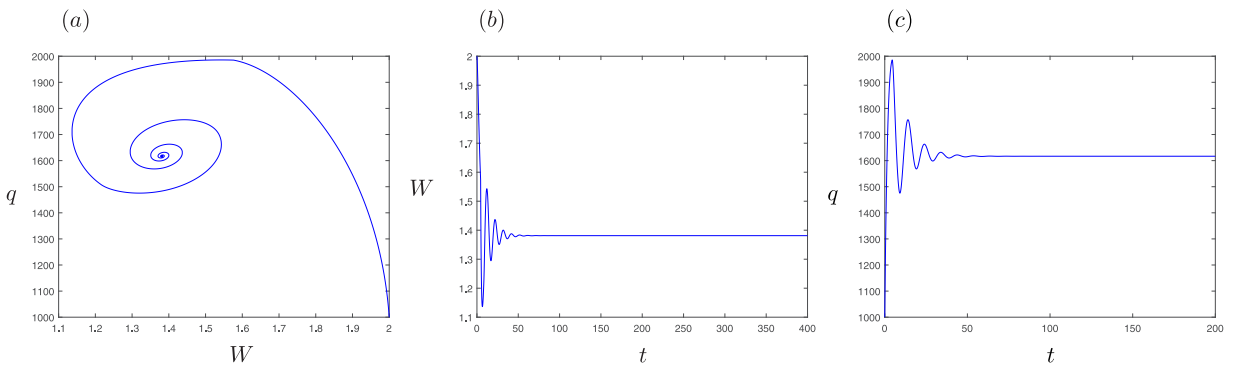


Fig. 10. (a) and (b), (c) correspond to the phase diagram and time histories of system (21) for $T_p = 1.95$, respectively.

approximation of the Period-1 solution for the parameter $T_p = 2.743$ by the HB-AFT method (see Appendix A.2). It is clearly that the HB-AFT result is in good agreement with that of the numerical solution by WinPP.

When the parameter T_p is varied further and increases to $T_p = 2.745$, and the initial functions are $(W(s), q(s)) = (2, 300)$, $s \in [-R_{max}, 0]$, there is another different stable Period-2 solution in Fig. 13(a), i.e., the stable Period-2 solution coexists with the stable Period-2 solution. When the parameter T_p continues to increase, a stable Period-4 solution occurs for $T_p \in (2.749, 2.7575)$ in Fig. 11(c). While, when the initial functions and parameter are $(W(s), q(s)) = (3, 800)$, $s \in [-R_{max}, 0]$, and $T_p = 2.75$, a stable Period-2 solution appears in Fig. 13(b), i.e., the stable Period-4 solution coexists with the stable Period-2 solution. With the increase of parameter T_p , for $T_p \in (2.762, 2.849)$, the Period Doubling sequence results in chaos eventually in Fig. 11(d). Corresponding to Figs. 11, 9(b) is the bifurcation diagram generated by Poincaré section with respect to T_p of the route of Period Doubling bifurcation to chaos.

4. Conclusions

In the present paper, the core work is to obtain the approximate analytical expressions of periodic solutions of the homogeneous AIMD/RED network congestion control systems with state-dependent round-trip delay via harmonic balance method with alternating frequency/time (HB-AFT). This task is very difficult, due to the existence of state-dependent delay. Compared with the traditional methods, the semi-analytical method called HB-AFT, in the process of solving the periodic response of the system, the response and the nonlinear function are set as harmonic solutions simultaneously, and the relationships between each order harmonic term are established directly according to the discrete time-frequency features of the system. It avoids the complicated integration of the Fourier coefficients of the nonlinear righthand of the system and requires fewer series expansion. Hence, this method translates the problem into a relatively simple one, it is highly efficient and applicable for the complex nonlinear system. Furthermore,

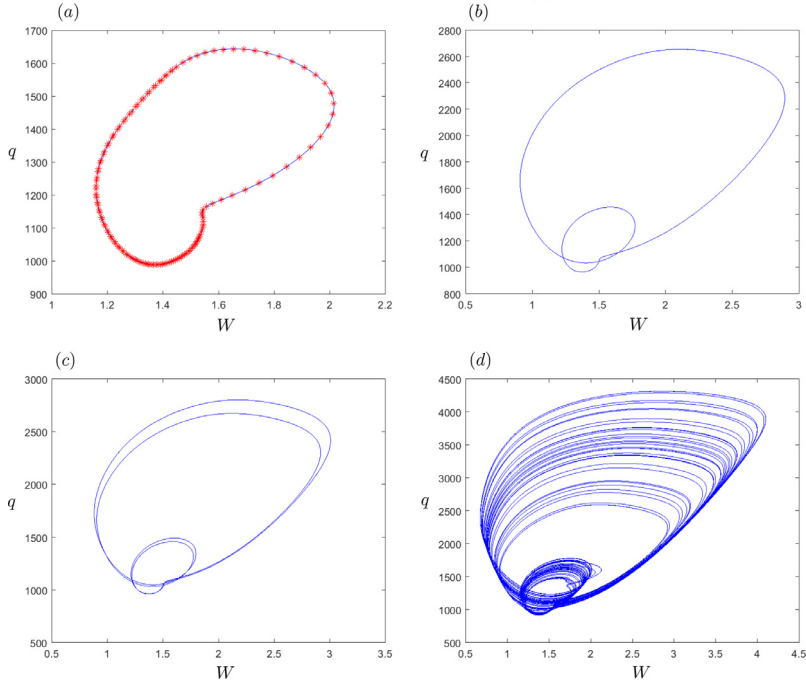


Fig. 11. Periodic and chaotic oscillations of the network congestion control system (21). (a) for $T_p = 2.71$, (b) for $T_p = 2.745$, (c) for $T_p = 2.75$, (d) for $T_p = 2.82$. And (a) is the comparison of numerical result (blue solid line) by WinPP with the result of the HB-AFT method (red *).

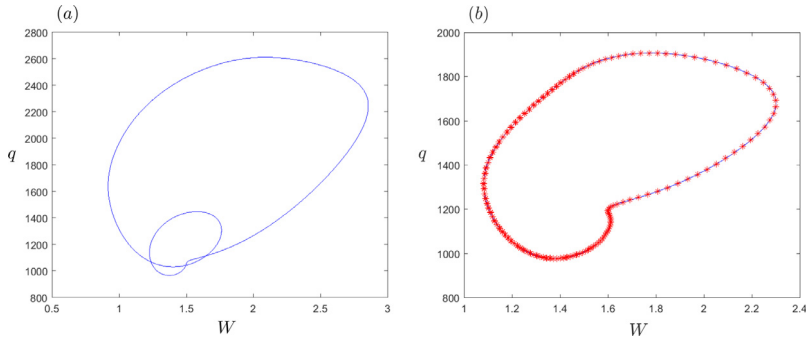


Fig. 12. The phenomenon of bi-stability of system (21) for $T_p = 2.743$. (a), (b) correspond to the initial functions $(W(s), q(s)) = (2, 1000)$ and $(W(s), q(s)) = (1, 700)$, $s \in [-R_{max}, 0]$, respectively. Additionally, (b) is the comparison between the phase diagram of the HB-AFT method (red *) and that of numerical result (blue solid line) by WinPP.

this method can be easily realized by MATLAB program. After the approximate analytical expressions of periodic solutions are obtained, we compare them with the numerical simulations results obtained by WinPP. They agree very well with each other. It indicates the validity, simplicity and effectiveness of the employed method. At the same time, for its modified version, the approximate analytical expressions of periodic solutions are achieved accurately by the HB-AFT method, and rich dynamical behaviors are discovered in this paper, for example, four kinds of bi-stability, i.e., the coexistence of chaos and Period-3 solution, that of Period-1 and Period-2 solutions, that of Period-2 and Period-2 solutions, that of Period-4 and Period-2 solutions are found. And we also discover a route to chaos, i.e., Period Doubling bifurcation to chaos, and the window of Period-3 to chaos, with the variation of T_p . Therefore, it can be discovered that the variation of parameter is significant to the dynamical behaviors. The

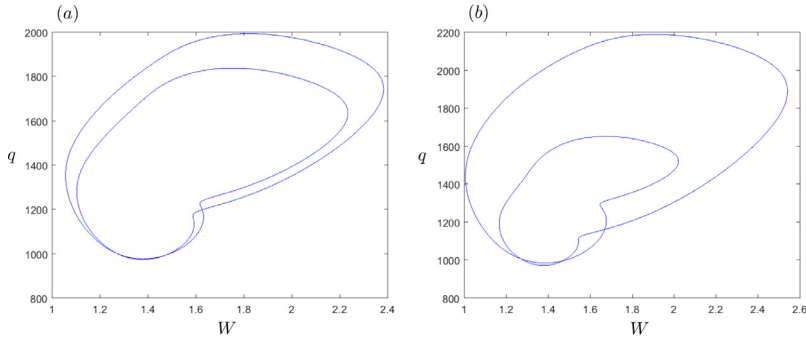


Fig. 13. The phase diagrams of system (21). (a), (b) correspond to the initial functions $(W(s), q(s)) = (2, 300)$, $s \in [-R_{max}, 0]$, the parameter $T_p = 2.745$, and $(W(s), q(s)) = (3, 800)$, $s \in [-R_{max}, 0]$, the parameter $T_p = 2.75$, respectively.

analytical approximation expressions of the Period- m solution are not obtained by the HB-AFT method, and will be considered in the further work.

As well known, the periodic and chaotic oscillations may lead to end-to-end service quality decline, loss of information and even result in collapse. Hence, in order to achieve the desired network performance, these bad phenomena found in this paper should be avoided. The obtained results provide a reference for the formulation of control strategy and they can be avoided by selecting the parameters properly.

Acknowledgments

The authors would like to acknowledge the financial support for this research via the Natural National Science Foundation of China (Nos. 11972327, 11372282 and 10702065). They also thank the reviewers for their valuable reviews and kind suggestions.

Appendix

A.1.

For the first set of parameters in Section 2.3, the program is as follows:

```
# numerical simulations of state-dependent delay systems
# declare all the parameters
p T_p = 0.7225, C = 1000, N = 500, alpha = 1, beta = 0.5, k1 = 0.002
# define the right-hand sides, delaying W by tau, i.e., the delay term is represented by delay(W,tau)
```

$$\begin{aligned} tau &= T_p + \frac{q(t)}{C} \\ \frac{dW(t)}{dt} &= \frac{\alpha}{T_p + q(t)/C} - \frac{2(1-\beta)*W(t)*delay(W,tau)*k*delay(q,tau)}{(1+\beta)*(T_p+delay(q,tau)/C)} \\ \frac{dq(t)}{dt} &= \frac{N*W(t)}{T_p + q(t)/C} - C \end{aligned}$$

```
@ total = 1000, xhi = 40, ylo = 0, yhi = 1, maxdelay = 1000, maxstor = 10000000, bound = 10000000, dt = 0.0001
```

```
# done
```

```
d
```

A.2.

According to the analysis in Section 2.2, we can get the Fourier coefficients and response frequency. So the analytical approximation of the Period-1 solution obtained by the HB-AFT method can be presented as follows for $T_p = 1.3$,

$$\begin{aligned} W(t) &\approx [0.0031 - 0.0010 \sin(\omega t) + 0.0002 \cos(2\omega t) - 0.0002 \sin(2\omega t) \\ &\quad - 0.0001 \cos(3\omega t) - 0.0001 \sin(3\omega t)] \times 10^3, \\ q(t) &\approx [1.2377 + 0.2144 \cos(\omega t) - 0.0867 \sin(\omega t) + 0.0246 \cos(2\omega t) \\ &\quad + 0.0192 \sin(2\omega t) + 0.0060 \cos(3\omega t) - 0.0074 \sin(3\omega t) \\ &\quad + 0.0021 \cos(4\omega t) - 0.0007 \sin(4\omega t) + 0.0001 \cos(5\omega t) \\ &\quad + 0.0001 \cos(6\omega t) - 0.0001 \sin(6\omega t)] \times 10^3, \end{aligned}$$

where the response frequency is $\omega = 0.7$.

On the basis of the previous analysis in Section 2.2, the Fourier coefficients and response frequency can be obtained. Hence, for $T_p = 2.71$, the analytical approximation of the Period-1 solution obtained by the HB-AFT method reads,

$$\begin{aligned} W(t) &\approx [0.0015 - 0.0003 \sin(\omega t) - 0.0001 \sin(2\omega t)] \times 10^3, \\ q(t) &\approx [1.2741 + 0.2859 \cos(\omega t) - 0.1370 \sin(\omega t) + 0.0444 \cos(2\omega t) \\ &\quad - 0.0280 \sin(2\omega t) - 0.0185 \cos(3\omega t) - 0.0120 \sin(3\omega t) \\ &\quad - 0.0081 \cos(4\omega t) + 0.0075 \sin(4\omega t) + 0.0021 \cos(5\omega t) \\ &\quad + 0.0017 \sin(5\omega t) + 0.0003 \cos(6\omega t) - 0.0010 \sin(6\omega t) \\ &\quad - 0.0001 \cos(7\omega t) + 0.0001 \cos(8\omega t) - 0.0002 \sin(8\omega t) \\ &\quad - 0.0002 \cos(9\omega t) - 0.0001 \sin(9\omega t) + 0.0002 \sin(10\omega t) \\ &\quad + 0.0001 \cos(11\omega t)] \times 10^3, \end{aligned}$$

where the response frequency is $\omega = 0.5$.

According to the analysis of Section 2.2, we can obtain the Fourier coefficients and response frequency. Therefore, for $T_p = 2.743$, the analytical approximation of the Period-1 solution obtained by the HB-AFT method is,

$$\begin{aligned} W(t) &\approx [0.0016 - 0.0005 \sin(\omega t) - 0.0001 \cos(2\omega t) - 0.0001 \sin(2\omega t) \\ &\quad - 0.0001 \cos(3\omega t) + 0.0001 \sin(3\omega t)] \times 10^3, \\ q(t) &\approx [1.3812 + 0.4042 \cos(\omega t) - 0.1947 \sin(\omega t) + 0.0639 \cos(2\omega t) \\ &\quad - 0.0407 \sin(2\omega t) - 0.0275 \cos(3\omega t) - 0.0169 \sin(3\omega t) \\ &\quad - 0.0107 \cos(4\omega t) + 0.0105 \sin(4\omega t) + 0.0023 \cos(5\omega t) \\ &\quad + 0.0019 \sin(5\omega t) + 0.0002 \cos(6\omega t) - 0.0007 \sin(6\omega t) \\ &\quad + 0.0005 \cos(7\omega t) + 0.0001 \sin(7\omega t) + 0.0002 \cos(8\omega t) \\ &\quad - 0.0007 \sin(8\omega t) - 0.0006 \cos(9\omega t) - 0.0001 \sin(9\omega t) \\ &\quad + 0.0003 \sin(10\omega t) + 0.0001 \cos(11\omega t) - 0.0001 \sin(11\omega t)] \times 10^3, \end{aligned}$$

where the response frequency is $\omega = 0.5$.

References

- [1] V. Jacobson, Congestion avoidance and control, ACM SIGCOMM Comput. Commun. Rev. 18 (1988) 314–329.
- [2] S. Floyd, V. Jacobson, Random early detection gateways for congestion avoidance, IEEE/ACM Trans. Netw. 1 (4) (1993) 397–413.
- [3] S. Athuraliya, S. Low, V.H. Li, Q. Yin, REM: active queue management, IEEE Netw. 15 (2001) 48–53.
- [4] S.T. Guo, X.F. Liao, C.D. Li, Stability and Hopf bifurcation analysis in a novel congestion control model with communication delay, Nonlinear Anal. Real World Appl. 9 (4) (2008) 1292–1309.
- [5] D.W. Ding, X.M. Qin, T.T. Wu, N. Wang, D. Liang, Hopf bifurcation control of congestion control model in a wireless access network, Neurocomputing 144 (2014) 159–168.

- [6] F.S. Gentile, J.L. Moiola, E.E. Paolini, Nonlinear dynamics of internet congestion control: A frequency-domain approach, *Commun. Nonlinear Sci. Numer. Simul.* 19 (4) (2014) 1113–1127.
- [7] J.S. Wang, R.X. Yuan, Z.W. Gao, et al., Hopf bifurcation and uncontrolled stochastic traffic induced chaos in an RED-AQM congestion control system, *Chin. Phys. B* 20 (9) (2011) 090506.
- [8] S. Zhang, J. Xu, Oscillatory dynamics induced by time delay in an internet congestion control model with ring topology, *Appl. Math. Comput.* 218 (22) (2012) 11033–11041.
- [9] J. Xu, L. Pei, Advances in dynamics for delayed systems, *Adv. Mech.* 36 (1) (2006) 17–30.
- [10] B.D. Hassard, N.D. Kazarinoff, Y.H. Wan, *Theory and Applications of Hopf Bifurcation*, Cambridge University Press, Cambridge, 1981.
- [11] S.L. Das, A. Chatterjee, Multiple scales without center manifold reductions for delay differential equations near Hopf bifurcations, *Nonlinear Dynam.* 30 (4) (2002) 323–335.
- [12] W. Zhang, T. Liu, A. Xi, et al., Resonant responses and chaotic dynamics of composite laminated circular cylindrical shell with membranes, *J. Sound Vib.* 423 (4) (2018) 65–99.
- [13] L. Pei, S. Wang, M. Wiercigroch, Analysis of hopf bifurcations in differential equations with state-dependent delays via multiple scales method, *ZAMM - J. Appl. Math. Mech. / Z. Angew. Math. Mech.* (2017).
- [14] J. Xu, K.W. Chung, A perterbation-incremental scheme for studying hopf bifurcation in delayed differential systems, *Sci. China* 52 (3) (2009) 698–708.
- [15] N. Macdonald, Harmonic balance in delay-differential equations, *J. Sound Vib.* 186 (1995) 649–656.
- [16] G.R. Itoivich, J.L. Moiola, On period doubling bifurcations of cycles and the harmonic balance method, *Chaos Soliton Fract.* 27 (2006) 647–665.
- [17] L. Xie, S. Baguet, B. Prabel, et al., Bifurcation tracking by Harmonic Balance Method for performance tuning of nonlinear dynamical systems, *Mech. Syst. Signal Process.* 88 (2017) 445–464.
- [18] E.H. Dowell, K.C. Hall, Modeling of fluid–structure interaction, *Annu. Rev. Fluid Mech.* 33 (1) (2001) 445–490.
- [19] R. Ju, W. Fan, et al., A modified two-timescale incremental harmonic balance method for steady-state quasi-periodic responses of nonlinear systems, *J. Comput. Nonlinear Dyn.* 12 (5) (2017) 051007.
- [20] A.R. Aghothama, S.N. Arayanan, Bifurcation and chaos in geared rotor bearing system by incremental harmonic balance method, *J. Sound Vib.* 226 (3) (1999) 469–492.
- [21] J.H. Shen, K.C. Lin, S.H. Chen, et al., Bifurcation and route-to-chaos analysis for Mathieu-Duffing oscillator by the incremental harmonic balance method, *Nonlinear Dynam.* 52 (4) (2008) 403–414.
- [22] A.C.J. Luo, *Regularity and Complexity in Dynamical Systems*, Springer, New York, 2012, pp. 49–59.
- [23] S. Yamauchi, The nonlinear vibration of flexible rotors, 1st report, development of a new analysis technique, *Trans. Jpn. Soc. Mech. Eng. Ser. C* 49 (446) (1983) 1862–1868.
- [24] Y.B. Kim, S.T. Noah, Quasi-periodic response and stability analysis for a non-linear jeffcott rotor, *J. Sound Vib.* 190 (2) (1996) 239–253.
- [25] Y.B. Kim, S.T. Noah, Stability and bifurcation analysis of oscillators with piecewise-linear characteristics: a general approach, *Trans. ASME, J. Appl. Mech.* 58 (2) (1991) 545–553.
- [26] Z. Zhang, Y. Chen, Harmonic balance method with alternating frequency/time domain technique for nonlinear dynamical system with fractional exponential, *Appl. Math. Mech.* 35 (4) (2014) 423–436.
- [27] T.C. Yuan, J. Yang, L.Q. Chen, A harmonic balance approach with alternating frequency/time domain progress for piezoelectric mechanical systems, *Mech. Syst. Signal Process.* 120 (2019) 274–289.
- [28] V. Misra, W.B. Gong, D. Towsley, Fluid-based analysis of a network of AQM routers supporting TCP flows with an application to RED, *Comput. Commun. Rev.* 30 (4) (2000) 151–160.
- [29] L. Wang, L. Cai, X. Liu, et al., Stability and TCP-friendliness of AIMD/RED systems with feedback delays, *Comput. Netw.* 51 (15) (2007) 4475–4491.
- [30] C.V. Hollot, Y. Chait, Nonlinear stability analysis for a class of TCP/AQM networks, in: Proceedings of the 40th IEEE Conference on Decision and Control, Vol. 3, IEEE, 2001, pp. 2309–2314.
- [31] L. Liu, E.H. Dowell, K.C. Hall, A novel harmonic balance analysis for the van der pol oscillator, *Int. J. Non-Linear Mech.* 42 (1) (2007) 2–12.
- [32] S. Zhang, J. Xu, K.W. Chung, On the stability and multi-stability of a tcp/red congestion control model with state-dependent delay and discontinuous marking function, *Commun. Nonlinear Sci. Numer. Simul.* 22 (1–3) (2015) 269–284.
- [33] G.W. Howell, J. Baillieul, Simple controllable walking mechanisms which exhibit bifurcations, in: IEEE Conference on Decision and Control, IEEE, 1998.